ROXAS: a new spectral code for isolated neutron star gravitational wave signal.

Gaël Servignat, Santiago Jaraba, Jérôme Novak, Micaela Oertel

servignat@apc.in2p3.fr, santiago.jaraba-gomez@astro.unistra.fr, jerome.novak@astro.unistra.fr, micaela.oertel@astro.unistra.fr

GdR Ondes Gravitationnelles: Réunion du groupe de travail Objets Compacts
September 17, 2025

Table of Contents

Table of Contents

Context

- Core collapse supernovae and binary merger simulations in General Relativity (GR) have gone under tremendous progress during the last $\sim$25 years.
- Shibata and Uryu: first 3D binary neutron star (NS) merger simulation [Shibata and Uryū, 2000].
- Valencia formulation [Banyuls et al., 1997; Font, 2008]: conservative formulation of GR-hydro equations.
- Development of high-resolution shock capturing (HSRC) methods.
- Numerical Relativity (NR) simulation of compact binary mergers: waveforms of inspiral + merger + ringdown.
- Next two decades: post-O5 runs of LIGO-Virgo-Kagra + Einstein Telescope & Cosmic Explorer, sensitivity increased in the kHz band.

Hydrodynamics

- Most hydrodynamical codes rely on conserved variables [Banyuls et al., 1997; Font, 2008].
- Different discretisation: finite volume [Cipolletta et al., 2021], Smooth Particle Hydrodynamics [Rosswog and Diener, 2021], spectral methods [Hébert et al., 2018].
- Allows the treatment of shocks.
- Inspiral + merger simulations possible.
- Conserved $\leftrightarrow$ physical (*primitive*) variables computationally expensive.
- Only $\sim$500 merger simulations in two decades: too few for a parametric study.

Goal

Writing a full-GR, full non-linear neutron star evolution code for post-merger phase.

- Final goal: run simulations of a post-merger hypermassive neutron star with 3-parameter equations of state (EoS), perform a parametric study by varying the EoS.
- Test beds in spherical symmetry with barotropic EoS.
- Axisymmetric and non-axisymmetric frequency extraction with barotropic EoS.
- Waveform extraction (gravitational waves signal).

We consider a perfect fluid of baryons carried by a timelike unitary 4-velocity u^ν:

$$T^{\mu\nu} = (e+p)u^\nu u^\mu + p g^{\mu\nu}$$

with e the total internal energy, p the fluid pressure, $g^{\mu\nu}$ the metric which is decomposed in the 3+1 formalism:

$$g_{\mu\nu}\mathrm{d}x^\mu \mathrm{d}x^\nu := -N^2\mathrm{d}t^2 + \gamma_{ij}(\mathrm{d}x^i + \beta^i \mathrm{d}t)(\mathrm{d}x^j + \beta^j \mathrm{d}t)$$

with N the lapse function, β^i the shift vector and γ_{ij} the 3-metric.

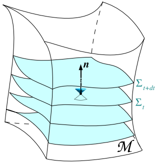

Figure: 3+1 foliation in spacelike hypersurfaces

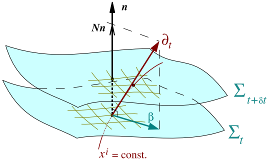

Figure: Illustration of the lapse and the shift

Physical variables are called "primitive" variables:

- e the energy density, p the pressure
- n_B the baryon number density
- m_B a baryon mass
- $H = \ln\left(\frac{e+p}{m_B n_B}\right)$ the log-enthalpy
- U_i the Eulerian velocity field
- v_i the coordinate velocity field
- c_s the sound speed

Table of Contents

Conservative variables

The variables $D = m_B n_B \Gamma^2$, $S_j = (e+p)\Gamma^2 U_j$ and $\tau = (e+p)\Gamma^2 - p$, with $\Gamma = (1 - U_i U^i)^{-1/2}$, are conserved in the sense that $\mathbf{u} = (D, S_j, \tau)$ obeys an equation that looks like

$$\partial_t \mathbf{u} + \mathrm{div}(F(\mathbf{u})) = \mathrm{source}$$

but the knowledge of e, p, U_i is compulsory to solve Einstein equations to compute the metric. **Recovery procedures are needed to recover the primitive variables in multiple steps of NR codes and account for a significant part of the computation:**

- Solving for the metric.
- Solving for the Riemann problems in each grid cell at each time step.

New set of equations using primitive variables [Servignat et al., 2023]

From the principles of stress-energy and baryon number conservation:

$$\nabla_\mu (n_B u^\mu) = 0, \ \nabla_\mu T^{\mu\nu} = 0,$$

the following holds for a barotropic, non-reactive perfect fluid with K_{ij} the extrinsic curvature tensor:

$$\begin{aligned}
\partial_t U_i = &-v^j D_j U_i - D_i N - \frac{N}{\Gamma^2}\left(D_i H - \frac{\Gamma^2(1-c_s^2)}{\Gamma^2 - c_s^2(\Gamma^2-1)} U_i U^j D_j H\right) \\
&+ U_j D_i \beta^j + U_i U^j D_j N \\
&+ \frac{N c_s^2}{\Gamma^2 - c_s^2(\Gamma^2-1)} U_i D_j U^j + \frac{N\Gamma^2(c_s^2-1)}{\Gamma^2 - c_s^2(\Gamma^2-1)} U_i U^j U^l K_{jl} \\
\partial_t H = &-v^i D_i H - c_s^2 N \frac{\Gamma^2}{\Gamma^2 - c_s^2(\Gamma^2-1)}\left[U^i U^j K_{ij} - \frac{U^i}{\Gamma^2} D_i H + D_i U^i\right]
\end{aligned}$$

This new set of equations is **covariant** within the 3+1 formalism.

e, p, c_s are recovered in a single call to the EoS **(no iteration)**.

New set of equations using primitive variables [Servignat et al., 2023]

From the principles of stress-energy and baryon number conservation:

$$\nabla_\mu (n_B u^\mu) = 0, \; \nabla_\mu T^{\mu\nu} = 0,$$

the following holds for a barotropic, non-reactive perfect fluid with K_{ij} the extrinsic curvature tensor:

$$\begin{aligned}
\partial_t U_i = & -v^j D_j U_i - D_i N - \frac{N}{\Gamma^2}\left(D_i H - \frac{\Gamma^2(1-c_s^2)}{\Gamma^2 - c_s^2(\Gamma^2-1)} U_i U^j D_j H \right) \\
& + U_j D_i \beta^j + U_i U^j D_j N \\
& + \frac{N c_s^2}{\Gamma^2 - c_s^2(\Gamma^2-1)} U_i D_j U^j + \frac{N\Gamma^2(c_s^2-1)}{\Gamma^2 - c_s^2(\Gamma^2-1)} U_i U^j U^l K_{jl} \\
\partial_t H = & -v^i D_i H - c_s^2 N \frac{\Gamma^2}{\Gamma^2 - c_s^2(\Gamma^2-1)} \left[U^i U^j K_{ij} - \frac{U^i}{\Gamma^2} D_i H + D_i U^i \right]
\end{aligned}$$

This new set of equations is **covariant** within the 3+1 formalism.

e, p, c_s are recovered in a single call to the EoS **(no iteration)**.

Table of Contents

ROXAS: Numerical ingredients [Servignat and Novak, 2025]

ROXAS: **R**elativistic **O**scillations of non-a**X**isymmetric neutron st**A**r**S**

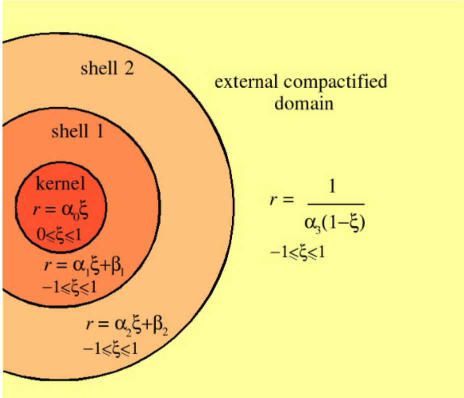

Figure: Metric grid: spherical numerical domains in LORENE.

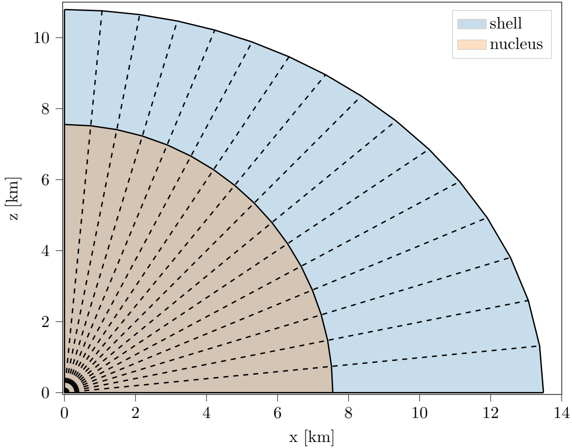

Figure: Hydro grid: deformed external domain

Table of Contents

Validation of the code

Test beds in spherical symmetry [Servignat et al., 2023]:

- Migration test.
- Collapse to a black hole.
- Spherically symmetric oscillations + frequency extraction (not shown here).
- Convergence tests (not shown here).

Non-spherically symmetric simulations [Servignat and Novak, 2025]:

- BU sequence: set of rigidly rotating polytropic NS.
- B sequence: set of differentially rotating polytropic NS.
- GW extraction with quadrupole formula.
- Frequency extraction on $Y_{\ell m}$ decomposition of $R(t)$.

Validation of the relativistic code: migration test [Servignat et al., 2023]

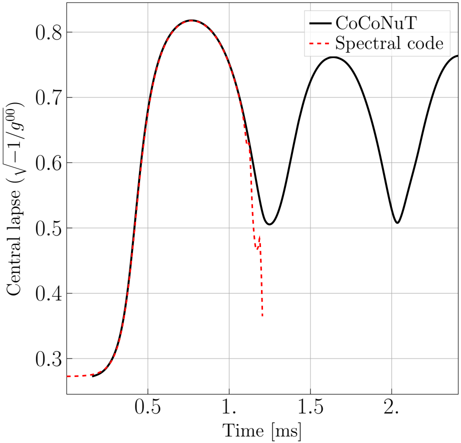

Figure: Central lapse.

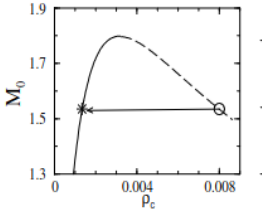

Figure: Migration test principle.

- Shock formation during the oscillations
- Gibbs phenomenon: the spectral code terminates.
- CoCoNuT: finite volume, high-resolution shock capturing techniques.
- 10s (spectral code) vs 6min (CoCoNuT).

Validation of the relativistic code: gravitational collapse [Servignat et al., 2023]

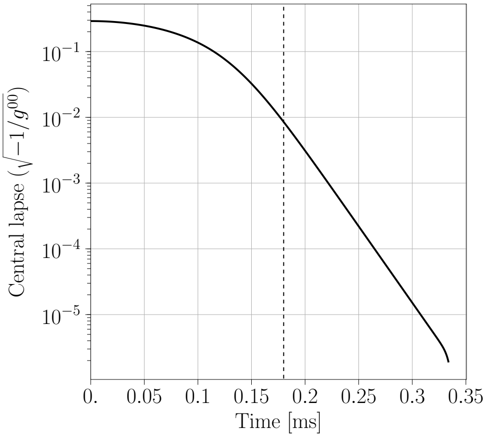

→ tests the strong gravity regime.

- Central lapse down to a few 10^{-6}.
- Freezing of the hydro quantities (maximal slicing).
- Apparent Horizon appearing around 0.18ms (dashed vertical line).

Table of Contents

GW extraction: stress formula

- Quadrupole formula:

$$h_{ij}^{TT}(\boldsymbol{x}, t) = \frac{2\mathcal{G}}{c^4 r} P_{ij}^{kl}(\boldsymbol{n}) \ddot{Q}_{kl}\left(t - \frac{r}{c}\right)$$

- First derivative transformed into [Blanchet et al., 1990]:

$$\frac{\mathrm{d}}{\mathrm{d}t} Q_{ij} = \int_{\mathbb{R}^3} \rho^* \left(x_i v_j + x_j v_i - \frac{2}{3}\delta_{ij} x_k v^k\right) \mathrm{d}^3 x,$$

$+$ backwards finite-differences scheme for second time derivative.

- Plus/cross polarisation decomposition:

$$h_{ij}^{TT}(\boldsymbol{x}, t) = \frac{1}{r}\left(A_+ \hat{\boldsymbol{e}}_+ + A_\times \hat{\boldsymbol{e}}_\times\right)$$

where

$$\hat{\boldsymbol{e}}_+ = \hat{\boldsymbol{e}}_\theta \otimes \hat{\boldsymbol{e}}_\theta - \hat{\boldsymbol{e}}_\varphi \otimes \hat{\boldsymbol{e}}_\varphi,$$

$$\hat{\boldsymbol{e}}_\times = \hat{\boldsymbol{e}}_\theta \otimes \hat{\boldsymbol{e}}_\varphi + \hat{\boldsymbol{e}}_\varphi \otimes \hat{\boldsymbol{e}}_\theta.$$

- Expression of A_+ and $A_\times$:

$$A_+^e = \frac{2\mathcal{G}}{c^4}\left(\ddot{Q}_{zz} - \ddot{Q}_{yy}\right), \; A_\times^e = -\frac{4\mathcal{G}}{c^4}\ddot{Q}_{yz}.$$

Numerical oscillations with ROXAS

BU4 model: rigidly rotating polytrope, $f_{\rm rot} = 673\,\mathrm{Hz}$.

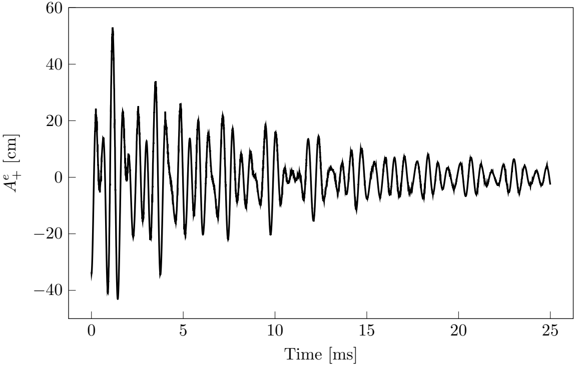

Figure: Waveform (BU4 model).

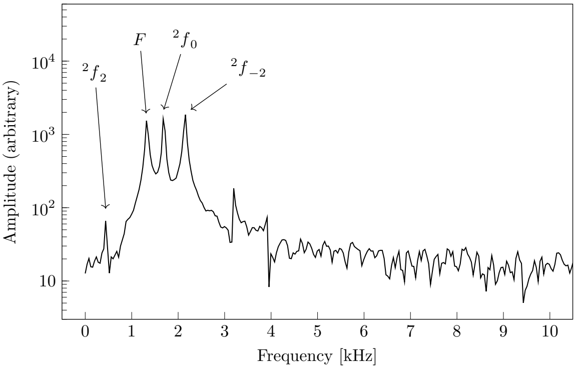

Figure: Spectrum (BU4 model).

Axisymmetric modes [Gaertig and Kokkotas, 2008; Dimmelmeier et al., 2006]

Model	$f_{\rm rot}$ [Hz]	M [$M_\odot$]	r_e [km]	$^2f_0$ [kHz]		Relative difference (%)	
				Cowling	CFC	Cowling	CFC
BU0	0	1.400	11.99	1.881	1.596	0.48	0.63
BU1	347	1.431	12.30	1.885	1.609	0.27	0.12
BU2	487	1.465	12.64	1.889	1.642	0.90	0.43
BU3	590	1.502	13.03	1.883	1.680	0.63	0.65
BU4	673	1.542	13.49	1.877	1.715	0.64	0.99
BU5	740	1.585	14.03	1.837	1.723	0.38	0.52
BU6	793	1.627	14.70	1.762	1.744	1.82	0.86
BU7	831	1.665	15.55	1.681	1.751	1.31	1.77
SLy4	191	1.361	9.34	2.400	1.964	$\times$	$\times$

Non-axisymmetric modes [Krüger et al., 2010; Krüger and Kokkotas, 2020]

Model	$f_{\rm rot}$ [Hz]	M [$M_\odot$]	r_e [km]	${}^2f_{-2}$ [kHz]		Relative difference (%)	
				Cowling	CFC	Cowling	CFC/GR
BU0	0	1.400	11.99	1.881	1.565	0.00	0.83
BU1	347	1.431	12.30	2.259	1.953	0.09	0.56
BU2	487	1.465	12.64	2.364	2.052	0.09	0.10
BU3	590	1.502	13.03	2.443	2.123	0.61	0.24
BU4	673	1.542	13.49	2.473	2.153	0.57	0.09
BU5	740	1.585	14.03	2.480	2.158	0.44	1.44
BU6	793	1.627	14.70	2.477	2.143	0.40	1.82
BU7	831	1.665	15.55	2.396	2.105	1.88	3.94
SLy4	191	1.361	9.34	2.640	2.185	$\times$	3.7

Non-axisymmetric modes [Krüger et al., 2010; Krüger and Kokkotas, 2020]

Model	f_{rot} [Hz]	M [$M_\odot$]	r_e [km]	${}^2f_2$ [kHz]		Relative difference (%)	
				Cowling	CFC	Cowling	CFC/GR
BU0	0	1.400	11.99	1.881	1.565	0.00	0.83
BU1	347	1.431	12.30	1.367	1.080	0.51	0.09
BU2	487	1.465	12.64	1.121	0.840	0.98	0.48
BU3	590	1.502	13.03	0.918	0.640	0.09	0.63
BU4	673	1.542	13.49	0.721	0.451	1.66	1.11
BU5	740	1.585	14.03	0.520	0.280	2.69	4.64
BU6	793	1.627	14.70	0.348	0.130	2.01	12.3
BU7	831	1.665	15.55	0.163	×	11.0	×
SLy4	191	1.361	9.34	2.141	1.675	×	1.2

Differential rotation

Rotation profile: $\mathbf{v}(r,\theta) = \Omega(r,\theta) r \sin\theta \hat{\mathbf{e}}_\varphi$.

The quantity $F = u^t u_\varphi = F(\Omega)$ enters the first integral of motion.

KEH profile [Komatsu et al., 1989]:

$$F(\Omega) = A^2(\Omega_c - \Omega)$$

Uryu et al. profile [Uryū et al., 2017]:

$$\Omega(F) = \Omega_c(1 + (F/B^2\Omega_c)^p)/(1 + (F/A^2\Omega_c)^{p+q}$$

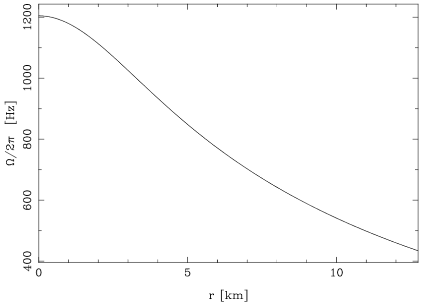

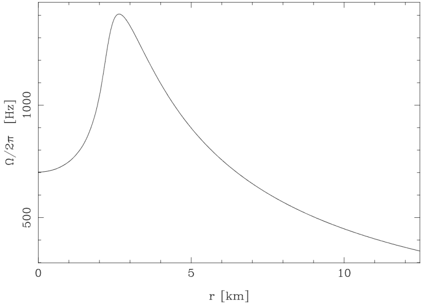

Differential rotation: waveforms with ROXAS

B4 model ($\Omega_c = 1205\,\mathrm{Hz}, \Omega_e = 434\,\mathrm{Hz}$):

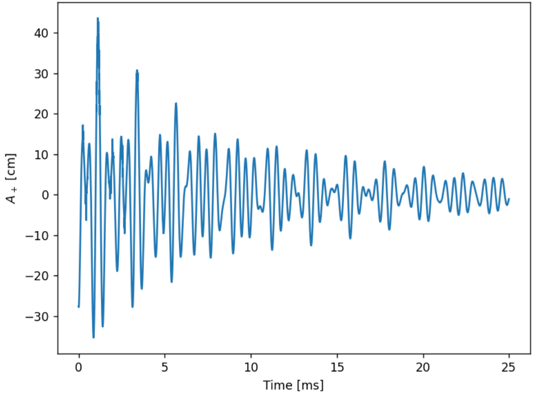

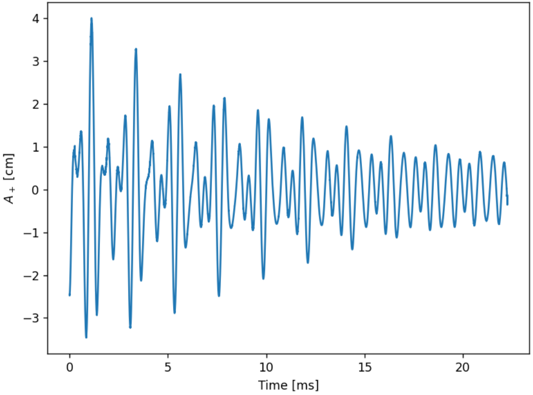

Differential rotation: spectra with ROXAS

B4 model ($\Omega_c = 1205\,\mathrm{Hz}, \Omega_e = 434\,\mathrm{Hz}$):

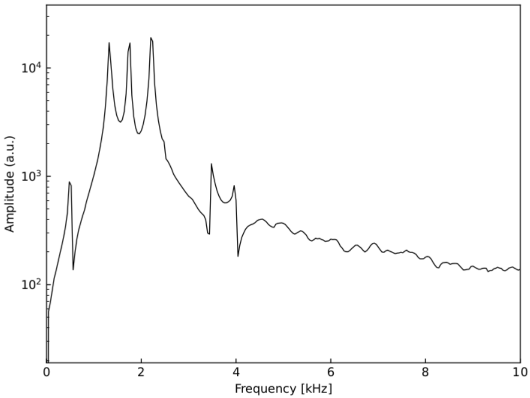

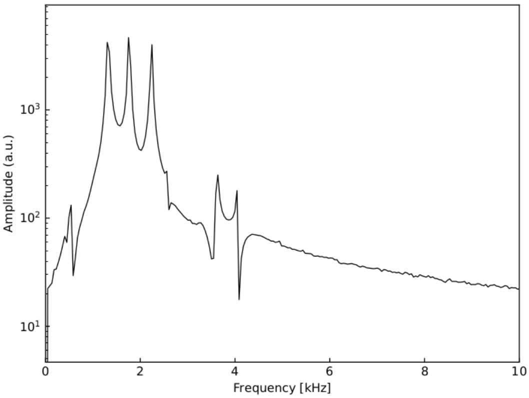

Differential rotation: frequency comparison (KEH profile) of ROXAS

Model	F	H_1	${}^2f_0$	${}^2f_2$	${}^2f_{-2}$	$F_{\rm ref}$	$H_{1,\rm ref}$	${}^2f_{0,\rm ref}$
B0	1.449	3.938	1.545	1.564	1.564	1.458	3.971	1.586
B1	1.427	3.904	1.602	1.115	1.939	1.407	3.927	1.628
B2	1.400	3.906	1.642	0.881	2.072	1.373	3.927	1.670
B3	1.363	3.930	1.685	0.681	2.159	1.332	3.964	1.709
B4	1.323	3.993	1.743	0.514	2.216	1.287	4.014	1.747
B5	1.293	4.040	1.775	0.320	2.276	1.237	4.072	1.789
B6	1.270	4.096	1.815	0.138	2.312	1.178	4.118	1.819
B7	1.237	4.147	1.865	-	2.352	1.077	4.179	1.854
B8	1.173	4.196	1.876	-	2.392	1.080	4.212	1.900
B9	1.148	4.164	1.936	-	2.450	0.945	4.469	1.917

Table: Frequencies and comparison to [Dimmelmeier et al., 2006].

Differential rotation: frequency comparison (KEH profile) of ROXAS

Model	F	H_1	$^2f_0$	$^2f_2$	$^2f_{-2}$	$F_{\rm ref}$	$H_{1,\rm ref}$	$^2f_{0,\rm ref}$
B0	1.449	3.938	1.545	1.564	1.564	1.458	3.971	1.586
B1	1.427	3.904	1.602	1.115	1.939	1.407	3.927	1.628
B2	1.400	3.906	1.642	0.881	2.072	1.373	3.927	1.670
B3	1.363	3.930	1.685	0.681	2.159	1.332	3.964	1.709
B4	1.323	3.993	1.743	0.514	2.216	1.287	4.014	1.747
B5	1.293	4.040	1.775	0.320	2.276	1.237	4.072	1.789
B6	1.270	4.096	1.815	0.138	2.312	1.178	4.118	1.819
B7	1.237	4.147	1.865	-	2.352	1.077	4.179	1.854
B8	1.173	4.196	1.876	-	2.392	1.080	4.212	1.900
B9	1.148	4.164	1.936	-	2.450	0.945	4.469	1.917

Table: Frequencies and comparison to [Dimmelmeier et al., 2006].

Table of Contents

Summary and outlook

- Development of a spectral code to evolve isolated neutron stars.
- New set of equations relying only on primitive variables.
- Non-barotropic oscillations studied in [Servignat et al., 2024].
- Extraction of non-axisymmetric mode frequencies with barotropic EoS (polytropes + one realistic EoS).
- GW signals extracted with quadrupole formula.

Summary and outlook

Assets:

- Very light code (3D simulations on laptop/office computer).
- Reasonable simulation time.
- No recovery procedure.
- Radius of the star followed by the grid.
- Very good frequency extraction (although CFC).
- Publicly available at `10.5281/zenodo.14849546`

Drawbacks:

- In practice: no shock treatment.
- Spectral methods are unforgiving.
- Only oscillations/post-merger phase.

Outlook:

- Perform longer simulations.
- Use nuclear equations of state.

Thank you!

Figure: Roxas, the eponymous cat **(left)**, Roxas City, Philippines' capital of seafood **(right)**.

Bibliography I

Francesc Banyuls, Jose A. Font, Jose Ma. Ibanez, Jose Ma. Marti, and Juan A. Miralles. Numerical $\{3 + 1\}$ General Relativistic Hydrodynamics: A Local Characteristic Approach. *Astrophysical Journal*, 476(1):221–231, February 1997. ISSN 0004-637X, 1538-4357. doi: 10.1086/303604. URL https://iopscience.iop.org/article/10.1086/303604.

Luc Blanchet, Thibault Damour, and Gerhard Schaefer. Post-Newtonian hydrodynamics and post-Newtonian gravitational wave generation for numerical relativity. *Monthly Notices of the Royal Astronomical Society*, 242:289–305, January 1990. ISSN 0035-8711. doi: 10.1093/mnras/242.3.289. URL https://ui.adsabs.harvard.edu/abs/1990MNRAS.242..289B. ADS Bibcode: 1990MNRAS.242..289B.

F Cipolletta, J V Kalinani, E Giangrandi, B Giacomazzo, R Ciolfi, L Sala, and B Giudici. Spritz: general relativistic magnetohydrodynamics with neutrinos. *Class. Quantum Grav.*, 38 (8):085021, April 2021. ISSN 0264-9381, 1361-6382. doi: 10.1088/1361-6382/abebb7. URL https://iopscience.iop.org/article/10.1088/1361-6382/abebb7.

Bibliography II

Isabel Cordero-Carrión, Pablo Cerdá-Durán, Harald Dimmelmeier, José Luis Jaramillo, Jérôme Novak, and Eric Gourgoulhon. Improved constrained scheme for the Einstein equations: An approach to the uniqueness issue. *Physical Review D*, 79(2):024017, January 2009. ISSN 1550-7998, 1550-2368. doi: 10.1103/PhysRevD.79.024017. URL `https://link.aps.org/doi/10.1103/PhysRevD.79.024017`.

Harald Dimmelmeier, Nikolaos Stergioulas, and José A. Font. Non-linear axisymmetric pulsations of rotating relativistic stars in the conformal flatness approximation. *Monthly Notices of the Royal Astronomical Society*, 368:1609–1630, June 2006. ISSN 0035-8711. doi: 10.1111/j.1365-2966.2006.10274.x. URL `https://ui.adsabs.harvard.edu/abs/2006MNRAS.368.1609D`. ADS Bibcode: 2006MNRAS.368.1609D.

Bibliography III

José A. Font. Numerical Hydrodynamics and Magnetohydrodynamics in General Relativity. *Living Reviews in Relativity*, 11:7, September 2008. doi: 10.12942/lrr-2008-7. URL `https://ui.adsabs.harvard.edu/abs/2008LRR....11....7F`. ADS Bibcode: 2008LRR....11....7F.

José A. Font, Tom Goodale, Sai Iyer, Mark Miller, Luciano Rezzolla, Edward Seidel, Nikolaos Stergioulas, Wai-Mo Suen, and Malcolm Tobias. Three-dimensional numerical general relativistic hydrodynamics. II. Long-term dynamics of single relativistic stars. *Physical Review D*, 65(8):084024, April 2002. ISSN 0556-2821, 1089-4918. doi: 10.1103/PhysRevD.65.084024. URL `https://link.aps.org/doi/10.1103/PhysRevD.65.084024`.

Erich Gaertig and Kostas D. Kokkotas. Oscillations of rapidly rotating relativistic stars. *Phys. Rev. D*, 78(6):064063, September 2008. ISSN 1550-7998, 1550-2368. doi: 10.1103/PhysRevD.78.064063. URL `https://link.aps.org/doi/10.1103/PhysRevD.78.064063`.

Bibliography IV

James B. Hartle and John L. Friedman. Slowly Rotating Relativistic Stars. VIII. Frequencies of the Quasi-Radial Modes of an $N = 3/2$ Polytrope. *Astrophysical Journal*, 196:653, March 1975. ISSN 0004-637X, 1538-4357. doi: 10.1086/153451. URL http://adsabs.harvard.edu/doi/10.1086/153451.

François Hébert, Lawrence E. Kidder, and Saul A. Teukolsky. General-relativistic neutron star evolutions with the discontinuous Galerkin method. *Physical Review D*, 98(4):044041, August 2018. ISSN 2470-0010, 2470-0029. doi: 10.1103/PhysRevD.98.044041. URL https://link.aps.org/doi/10.1103/PhysRevD.98.044041.

H. Komatsu, Y. Eriguchi, and I. Hachisu. Rapidly rotating general relativistic stars - I. Numerical method and its application to uniformly rotating polytropes. *Monthly Notices of the Royal Astronomical Society*, 237(2):355–379, March 1989. ISSN 0035-8711, 1365-2966. doi: 10.1093/mnras/237.2.355. URL https://academic.oup.com/mnras/article-lookup/doi/10.1093/mnras/237.2.355.

Bibliography V

Christian Krüger, Erich Gaertig, and Kostas D. Kokkotas. Oscillations and instabilities of fast and differentially rotating relativistic stars. *Phys. Rev. D*, 81(8):084019, April 2010. ISSN 1550-7998, 1550-2368. doi: 10.1103/PhysRevD.81.084019. URL https://link.aps.org/doi/10.1103/PhysRevD.81.084019.

Christian J. Krüger and Kostas D. Kokkotas. Dynamics of fast rotating neutron stars: An approach in the Hilbert gauge. *Phys. Rev. D*, 102(6):064026, September 2020. ISSN 2470-0010, 2470-0029. doi: 10.1103/PhysRevD.102.064026. URL https://link.aps.org/doi/10.1103/PhysRevD.102.064026.

S. Rosswog and P. Diener. SPHINCS_bssn: a general relativistic smooth particle hydrodynamics code for dynamical spacetimes. *Classical and Quantum Gravity*, 38:115002, June 2021. ISSN 0264-9381. doi: 10.1088/1361-6382/abee65. URL https://ui.adsabs.harvard.edu/abs/2021CQGra..38k5002R. ADS Bibcode: 2021CQGra..38k5002R.

Bibliography VI

Gaël Servignat, Jérôme Novak, and Isabel Cordero-Carrión. A new formulation of general-relativistic hydrodynamic equations using primitive variables. *Classical and Quantum Gravity*, 40(10):105002, May 2023. doi: 10.1088/1361-6382/acc828.

Gaël Servignat and Jérôme Novak. ROXAS: a new pseudospectral non-linear code for general relativistic oscillations of fast rotating isolated neutron stars. *Classical and Quantum Gravity*, 42(9):095015, May 2025. ISSN 0264-9381, 1361-6382. doi: 10.1088/1361-6382/adcd1e. URL `https://iopscience.iop.org/article/10.1088/1361-6382/adcd1e`.

Gaël Servignat, Philip J. Davis, Jérôme Novak, Micaela Oertel, and José A. Pons. One- and two-argument equation of state parametrizations with continuous sound speed for neutron star simulations. *Physical Review D*, 109(10):103022, May 2024. ISSN 2470-0010, 2470-0029. doi: 10.1103/PhysRevD.109.103022. URL `https://link.aps.org/doi/10.1103/PhysRevD.109.103022`.

Bibliography VII

Masaru Shibata and K. ōji Uryū. Simulation of merging binary neutron stars in full general relativity: $\Gamma=2$ case. *Physical Review D*, 61(6):064001, March 2000. doi: 10.1103/PhysRevD.61.064001.

Kōji Uryū, Antonios Tsokaros, Luca Baiotti, Filippo Galeazzi, Keisuke Taniguchi, and Shin'ichirou Yoshida. Modeling differential rotations of compact stars in equilibriums. *Physical Review D*, 96(10):103011, November 2017. ISSN 2470-0010, 2470-0029. doi: 10.1103/PhysRevD.96.103011. URL `https://link.aps.org/doi/10.1103/PhysRevD.96.103011`.

Frequency extraction principle

- Frequency extraction: spectrum computed with FFT algorithm on $R(t)$ then peak extraction.

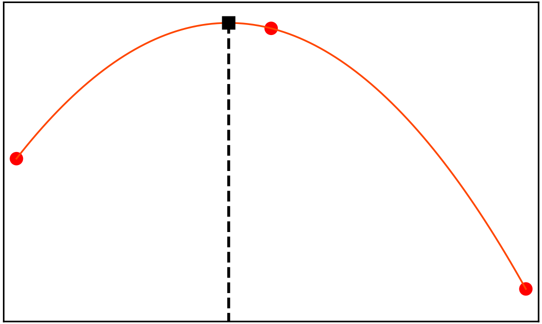

Figure: Frequency extraction principle.

EINSTEIN equations

Lapse, shift, and 3-metric entirely determine the geometry of $\mathcal{M}$:

$$g_{\alpha\beta} = \begin{pmatrix} g_{00} & g_j \\ g_i & g_{ij} \end{pmatrix} = \begin{pmatrix} -N^2 + \beta_k \beta^k & \beta_j \\ \beta_i & \gamma_{ij} \end{pmatrix}$$

$\rightarrow$ The 3+1 formalism allows for a **natural separation of time and space**.

Definition of matter terms:

$$\begin{aligned} E &= T_{\mu\nu} n^\mu n^\nu \text{ the matter energy density,} \\ p_\alpha &= -T_{\mu\nu} n^\mu \gamma^\nu_\alpha \text{ the matter momentum density,} \\ S_{\alpha\beta} &= T_{\mu\nu} \gamma^\mu_\alpha \gamma^\nu_\beta \text{ the matter stress tensor,} \end{aligned}$$

and $S_t = S_{\alpha\beta}\gamma^{\alpha\beta}$ and $T = T_{\alpha\beta} g^{\alpha\beta}$.

Conformal decomposition

Let $\boldsymbol{f}$ be a flat metric of signature $(+,+,+)$. $(\mathcal{M}, \boldsymbol{g})$ is asymptotically flat i.e. $\gamma = \boldsymbol{f}$ at spatial infinity.

$$\boxed{\Psi = \left(\frac{\gamma}{f}\right)^{1/12}} \gamma = \det(\gamma_{ij}),\ f = \det(f_{ij})$$

Using

$$\tilde{\gamma}_{ij} = \Psi^{-4}\gamma_{ij}$$

The EINSTEIN equations become (using the CFC: $\tilde{\gamma} = \boldsymbol{f}$):

$$\Delta\Psi = -2\pi\Psi^5 \left[E + \frac{1}{16\pi}K_{ij}K^{ij}\right]$$

$$\Delta(N\Psi) = 2\pi N\Psi^5 \left[E + 2S_t + \frac{7}{16\pi}K_{ij}K^{ij}\right]$$

$$\Delta\beta^i + \frac{1}{3}\bar{D}^i\bar{D}_j\beta^j = 16\pi N\Psi^4 p^i + 2\Psi^{10}K^{ij}\bar{D}_j\left(\frac{N}{\Psi^6}\right)$$

Conformal decomposition

Let $\boldsymbol{f}$ be a flat metric of signature $(+,+,+)$. $(\mathcal{M},\boldsymbol{g})$ is asymptotically flat i.e. $\boldsymbol{\gamma}=\boldsymbol{f}$ at spatial infinity.

$$\boxed{\Psi=\left(\frac{\gamma}{f}\right)^{1/12}}\ \gamma=\det(\gamma_{ij}),\ f=\det(f_{ij})$$

Using

$$\tilde{\gamma}_{ij}=\Psi^{-4}\gamma_{ij}$$

The EINSTEIN equations become (using the CFC: $\tilde{\boldsymbol{\gamma}}=\boldsymbol{f}$):

$$\Delta\Psi=-2\pi\Psi^{5}\left[E+\frac{1}{16\pi}K_{ij}K^{ij}\right]$$

$$\Delta(N\Psi)=2\pi N\Psi^5\left[E+2S_t+\frac{7}{16\pi}K_{ij}K^{ij}\right]$$

$$\Delta\beta^i+\frac{1}{3}\bar{D}^i\bar{D}_j\beta^j=16\pi N\Psi^4p^i+2\Psi^{10}K^{ij}\bar{D}_j\left(\frac{N}{\Psi^6}\right)$$

Uniqueness issue [Cordero-Carrión et al., 2009]

Additional conformal decomposition:

$$\hat{A}^{ij} = \Psi^{10} K^{ij};\ \hat{A}^{ij} \approx \bar{D}^i X^j + \bar{D}^j X^i - \frac{2}{3}\bar{D}_k X^k f^{ij}.$$

Starred quantities:

$$E^* = \Psi^6 E,\ S_t^* = \Psi^6 S_t,\ p_j^* = \Psi^6 p_j.$$

Leads to:

$$\begin{aligned}
\Delta X^i + \frac{1}{3}\bar{D}^i \bar{D}_j X^j =& 8\pi f^{ij} p_j^*, \\
\Delta \ln \Psi =& -2\pi \Psi^{-2} E^* - \Psi^{-8} \frac{f_{il} f_{jm} \hat{A}^{lm} \hat{A}^{ij}}{8} - D_i \ln \Psi D^i \ln \Psi, \\
\Delta N =& 4\pi N \Psi^{-2}(E^* + S_t^*) + N\Psi^{-8} f_{il} f_{jm} \hat{A}^{lm} \hat{A}^{ij} - 2 D_i \ln \Psi D^i N, \\
\Delta \beta^i + \frac{1}{3}\bar{D}^i \bar{D}_j \beta^j =& \bar{D}_j (2N\Psi^{-6} \hat{A}^{ij}).
\end{aligned}$$

Additional conformal decomposition:

$$\hat{A}^{ij} = \Psi^{10} K^{ij};\ \hat{A}^{ij} \approx \bar{D}^i X^j + \bar{D}^j X^i - \frac{2}{3}\bar{D}_k X^k f^{ij}.$$

Starred quantities:

$$E^* = \Psi^6 E,\ S_t^* = \Psi^6 S_t,\ p_j^* = \Psi^6 p_j.$$

Leads to:

$$\begin{aligned}
\Delta X^i + \frac{1}{3}\bar{D}^i \bar{D}_j X^j &= 8\pi f^{ij} p_j^*, \\
\Delta \ln \Psi &= -2\pi \Psi^{-2} E^* - \Psi^{-8} \frac{f_{il} f_{jm} \hat{A}^{lm} \hat{A}^{ij}}{8} - D_i \ln \Psi D^i \ln \Psi, \\
\Delta N &= 4\pi N \Psi^{-2}(E^* + S_t^*) + N\Psi^{-8} f_{il} f_{jm} \hat{A}^{lm} \hat{A}^{ij} - 2 D_i \ln \Psi D^i N, \\
\Delta \beta^i + \frac{1}{3}\bar{D}^i \bar{D}_j \beta^j &= \bar{D}_j (2N\Psi^{-6} \hat{A}^{ij}).
\end{aligned}$$

Validation of the relativistic code: frequency extraction [Servignat et al., 2023]

Table: Comparing the code and the literature.

	κ	γ	$H_c\,[c^2]$	$M\,[M_\odot]$	R [km]	Fund. [kHz]	1st ov. [kHz]	2nd ov. [kHz]
[Font et al., 2002]	100	2	0.2279	1.4	14.15	1.450	3.958	5.935
This work	100	2	0.2279	1.401	14.16	1.442	3.954	5.915
Relative difference						0.6%	0.1%	0.3%
[Hartle and Friedman, 1975]	7.308	5/3	6.720×10^{-2}	$\times$	$\times$	0.824	1.94	2.86
This work	7.308	5/3	6.720×10^{-2}	0.4866	16.49	0.823	1.95	2.86
Relative difference						0.1%	0.5%	0.0%

Table: COWLING approximation (fixing spacetime to initial value).

	κ	γ	$H_c\,[c^2]$	$M\,[M_\odot]$	R [km]	Fund. [kHz]	1st ov. [kHz]	2nd ov. [kHz]
[Font et al., 2002]	100	2	0.2279	1.4	14.15	2.696	4.534	6.346
This work	100	2	0.2279	1.401	14.16	2.685	4.548	6.339
Relative difference						0.4%	0.3%	0.1%

Validation of the relativistic code: convergence tests [Servignat et al., 2023]

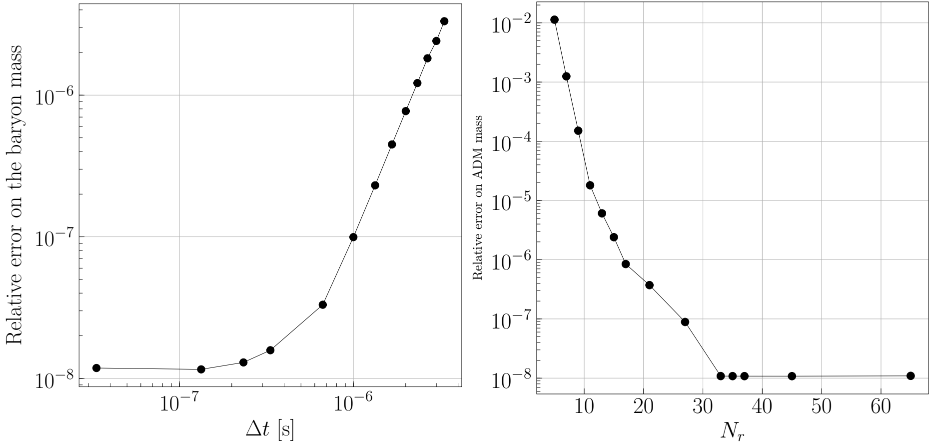

Figure: Convergence plots. Baryon mass, fixed number of grid points $N_r = 17$ (left). ADM mass, fixed value of the time step $\Delta t = 3.34 \times 10^{-7}\,\mathrm{s}$ (right).